GEOLOGY | THE GEOLOGICAL SOCIETY OF AMERICA®

https://doi.org/10.1130/G47365.1

Manuscript received 3 January 2020
Revised manuscript received 11 May 2020
Manuscript accepted 18 May 2020

Field evidence for coal combustion links the 252 Ma Siberian Traps with global carbon disruption

L.T. Elkins-Tanton[1], S.E. Grasby[2], B.A. Black[3,4], R.V. Veselovskiy[5,6], O.H. Ardakani[2] and F. Goodarzi[7]
[1]School of Earth and Space Exploration, Arizona State University, 781 Terrace Mall, Tempe, Arizona 95287, USA
[2]Geological Survey of Canada, Natural Resources Canada, 3303 33rd Street NW, Calgary, Alberta T2L 2A7, Canada
[3]Department of Earth and Atmospheric Science, City College of New York, 160 Convent Avenue, New York, New York 10031, USA
[4]Earth and Environmental Science, City University of New York Graduate Center, 365 Fifth Avenue, New York, New York, USA
[5]Institute of Physics of the Earth, Russian Academy of Sciences, Moscow 123242, Russia
[6]Geological Faculty, Lomonosov Moscow State University, Moscow 119991, Russia
[7]FG & Partners Ltd., 219 Hawkside Mews NW, Calgary, Alberta T3G 3J4, Canada

ABSTRACT

The Permian-Triassic extinction was the most severe in Earth history. The Siberian Traps eruptions are strongly implicated in the global atmospheric changes that likely drove the extinction. A sharp negative carbon isotope excursion coincides within geochronological uncertainty with the oldest dated rocks from the Norilsk section of the Siberian flood basalts. We focused on the voluminous volcaniclastic rocks of the Siberian Traps, relatively unstudied as potential carriers of carbon-bearing gases. Over six field seasons we collected rocks from across the Siberian platform, and we show here the first direct evidence that the earliest eruptions in the southern part of the province burned large volumes of a combination of vegetation and coal. We demonstrate that the volume and composition of organic matter interacting with magmas may explain the global carbon isotope signal and may have significantly driven the extinction.

INTRODUCTION

With loss of >90% of marine species, the Permian-Triassic extinction was the most severe in Earth history (Erwin, 2006). High-precision geochronology implicates Siberian Traps eruptions in the global environmental changes that caused the extinction (Wignall, 2001; Grasby et al., 2011; Burgess and Bowring, 2015; Burgess et al., 2017) and carbon cycle perturbation, including a sharp negative carbon isotope excursion that is a key feature of the mass-extinction interval (e.g., Payne and Clapham, 2012). This carbon isotope excursion coincides within geochronological uncertainty with the oldest dated rocks from the Norilsk section of the Siberian flood basalts (Burgess and Bowring, 2015).

Siberian Traps magmas were chambered within, and intruded through, the Tunguska sedimentary sequence (Il'yukhina and Verbitskaya, 1976). The Tunguska Basin varies between 3 and 12 km thick, and includes carbonates, evaporites, oil and gas, and coal (e.g., Svensen et al., 2018). Coal strata range in age from Carboniferous to Permian, with a cumulative coal thickness of ~100 m (Ryabov et al., 2014). Thermal metamorphism and combustion of coal, carbonates, and organic-rich shales produce significant CO_2 and CH_4, as well as carbonate metamorphism producing CO_2, in addition to the gases released by volcanics, all of which would have contributed to global warming (Retallack and Jahren, 2008; Svensen et al., 2009; Iacono-Marziano et al., 2012). However, the magnitude, tempo, and origin of carbon emissions during Siberian Traps magmatism have remained in question despite their critical atmospheric importance (Cui and Kump, 2015; Black et al., 2018).

The earliest volcanic deposits of the Siberian Traps include volcaniclastic rocks that overlie Paleozoic sedimentary rocks and underlie the main lava pile in the southern regions of the province (Naumov and Ankudimova, 1995). The thickest volcaniclastic rocks are near the town of Tura and farther south (Fig. 1). Near Tura, drill cores reveal >600 m of volcaniclastic rocks, grading directly into the earliest lavas of the flood basalts (Levitan and Zastoina, 1985). In the Maymecha-Kotuy region, the Pravoboyarsky Suite basal volcaniclastic sequence reaches a maximum thickness of 200–300 m (Fedorenko and Czamanske, 1997). Near Norilsk, the basal volcaniclastic sequences is typically only several meters thick.

The presence of coal fly ash layers at the end-Permian boundary in Arctic Canada provides tantalizing evidence for coal combustion at that time (Grasby et al., 2011). We examined the organic carbon content of the Siberian Traps rocks with a particular focus on early volcaniclastic rocks spanning the large igneous province (Table 1), from earliest eruptions to latest (here we are referring to the late-stage rocks of the Maymecha-Kotuy region), to provide a comprehensive assessment of organic-matter incorporation during magmatism. Here we give further evidence that Siberian Traps magmas intruded into and incorporated coal and organic material, and, for the first time, give direct evidence that the magmas also combusted large quantities of coal and organic matter during eruption.

METHODS AND RESULTS

Field Sampling

We sampled along a traverse north from Ust-Ilimsk along ~200 km of the Angara River, and a similar distance along the Nizhnyaya Tunguska River centering on Tura (Fig. 1). Almost every outcrop on these rivers consists of thick sequences of volcaniclastic rocks, which have been mapped in direct contact with upper Permian sedimentary rocks (Malich et al., 1974). Carbonized woody fragments as much as 10 cm in length were embedded in a number of outcrops on both the Angara and Nizhnyaya Tunguska Rivers (Black et al., 2015). No exposures of Permian and older coal layers were observed along either river. However, dolerite in a coal quarry near the Angara River in Ust-Ilimsk

CITATION: Elkins-Tanton, L.T., et al., 2020, Field evidence for coal combustion links the 252 Ma Siberian Traps with global carbon disruption: Geology, v. 48, p. , https://doi.org/10.1130/G47365.1

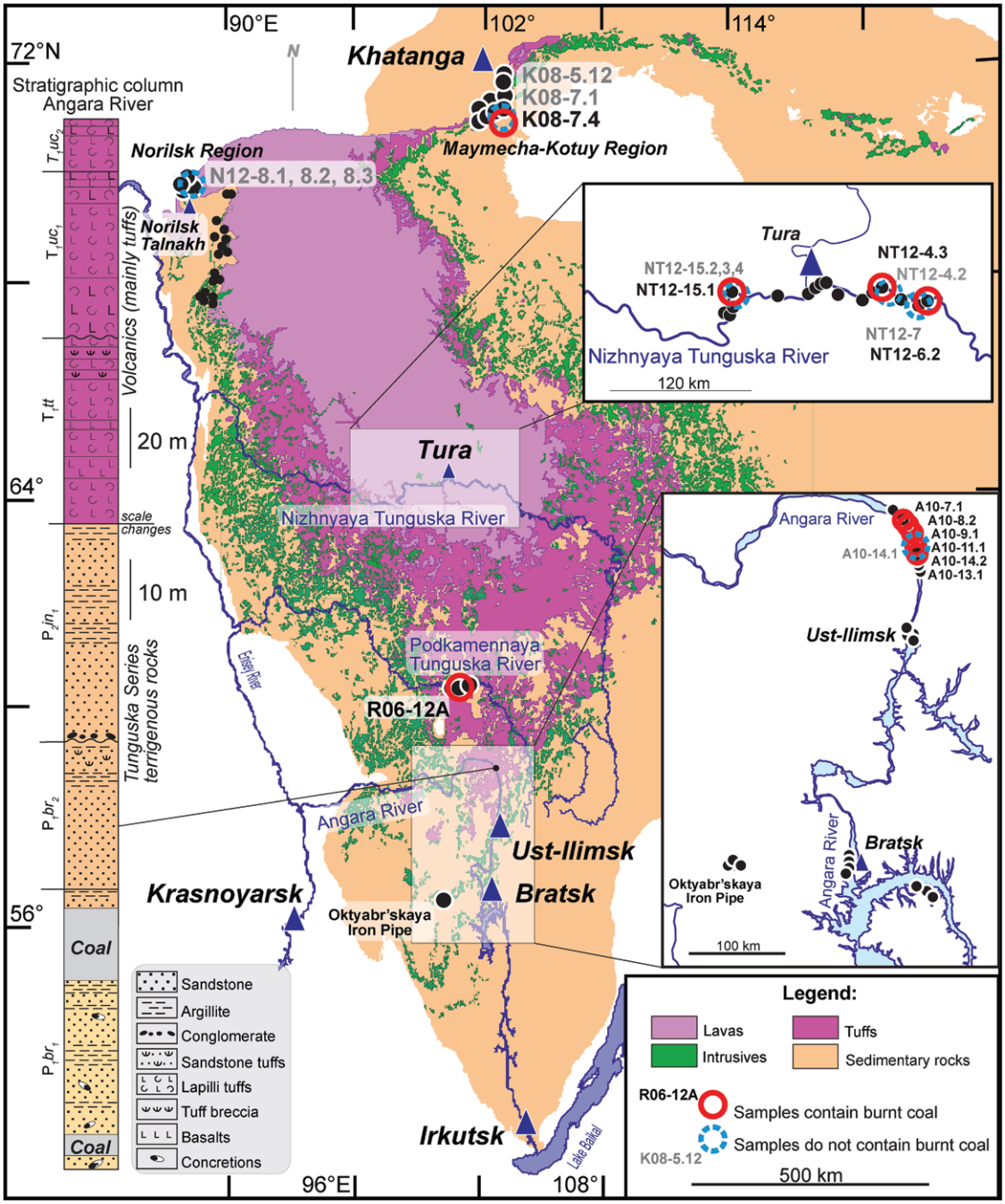

Figure 1. Map showing early southern volcaniclastics of the Siberian Traps that display abundant evidence for coal burning. Black dots mark sampling areas from the larger Siberian flood basalts and end-Permian extinction research project (funded under U.S. National Science Foundation grant EAR-0807585). Samples analyzed but with no coal found are labeled in gray with blue circles; those with red circles and black labels contain combusted, coked, or thermally altered coal. The majority of southern volcaniclastics analyzed contain coal, but only one from the northern Kotuy and Norilsk regions; in the intermediate Nizhnyaya Tunguska region, three out of eight samples contained coal. Map after Svensen et al. (2009) and Malich et al. (1974); stratigraphic column after Permyakov et al. (2012). On the stratigraphic column: P_1br_1 and P_1br_2—lower and upper parts of the Burguklinskaya Formation (Lower Permian), respectively; P_2in_1—lower part of the Inganbinskaya Formation (Middle Permian); T_1tt—Tutonchanskaya Formation (Lower Triassic); T_1uc_1 and T_1uc_2—lower and upper parts of the the Uchamskaya Formation (Lower Triassic), respectively.

contains vesicles filled with carbon-rich material, malleable with a fingernail (Fig. 2).

We examined 16 samples of volcaniclastic rocks from the Angara, Nizhnyaya Tunguska, and Podkamennaya Tunguska Rivers for carbon content, along with six samples from northern regions (Table 1; Fig. 1; detailed localities are provided in Figs. S3–S7 in the Supplemental Material[1]). These rocks have a range of whole-rock bulk carbon content of as much as 2.7 wt%, and total organic carbon (TOC) content from 0.01 to 1.16 wt% (Table 1; see the Supplemental Material). As context, TOC values in shales of >0.5 wt% have potential as a petroleum source rock (Peters and Cassa, 1994); the volcaniclastic rocks studied here may exceed the carbon threshold for an economically viable petrochemical source.

Characteristics of Burnt Coal and Organic Matter in Siberian Volcaniclastic Rocks

Samples were prepared as crushed-rock polished pellets and examined under reflected light (Table 1; Table S1 in the Supplemental Material). Of the 22 samples examined, 11 samples that span five geographically separated regions had visible large organic fragments enclosed in the rock matrix (Fig. 2) as well as organic macerals visible under the microscope (Figs. 3A–3N; Table S1). High values of random vitrinite reflectance (R_{or}) are indicative of higher thermal maturation of organic matter. The thermal maturity of the particles ranged from marginally mature to mature (R_{or} = 0.56%–0.83%), indicating the varying degree that organic matter was thermally altered by incorporation into the magma. We divided the organic particles into three general maceral types based on morphology and thermal maturation (Table 1).

Type 1 macerals are coal fragments within the volcaniclastic host rock that predominantly

[1]Supplemental Material. Methods and detailed location maps for samples. Please visit https://doi.org/10.1130/GEOL.S.12425381 to access the supplemental material, and contact editing@geosociety.org with any questions. Additional sample material is available from the corresponding author (L.T. Elkins-Tanton) at Arizona State University, Tempe, Arizona, USA.

TABLE 1. VOLCANICLASTIC SAMPLES FROM THE SIBERIAN TRAPS, WITH THEIR CARBON CONTENT AND COAL INTERACTION

Sample*	C#†	Bulk-rock carbon content (wt%)§	Total organic carbon (wt%)#	T1**	T2**	T3**	Sample description	Eruption *T*††	Figure§§	Latitude (°N)	Longitude (°E)
Nizhnyaya Tunguska River (pre-lava volcaniclastics, southern region)											
NT12-4.2	C-580294	1.52	1.16	N.D.	N.D.	N.D.	Lapilli tuff with abundant lithic clasts.	Possibly high temperature		64.11388	100.86677
NT12-4.3	C-580299	N.D.	47.8	95%	1%	4%	Organic chunk from a tuff.	N.D.	Figs. 3E, 3F	64.11388	100.86677
NT12-6.2	C-580293	0.18	0.39	80%	15%	5%	Lapilli tuff with primarily juvenile clasts.	N.D.	Figs. 3A–3D, 3L, 3 M, 3N; Figs. S2a–S2o	64.03910	102.30627
NT12-7	C-580292	0.32	0.44	N.D.	N.D.	N.D.	Tuff breccia with stringers of glass and angular juvenile clasts.	N.D.		64.16063	101.31985
NT12-15.1	C-580287	0.83	0.11	1%	19%	80%	Yellow-hued lapilli tuff at base of 100 m+ outcrop.	N.D.	Figs. S2p–S2u	64.16932	98.23712
NT12-15.2	C-597434	0.35	0.08	N.D.	N.D.	N.D.	Tuff breccia with abundant lithic clasts.	N.D.		64.16932	98.23712
NT12-15.3	C-597435	1.38	0.01	N.D.	N.D.	N.D.	Reddish lapilli tuff.	N.D.		64.16932	98.23712
NT12-15.4	C-580286	0.55	0.04	N.D.	N.D.	N.D.	Lapilli tuff.	N.D.		64.16932	98.23712
Norilsk Region (volcaniclastics early in the lava sequence, northern region)											
N12-8.1	C-580291	1.52	0.38	N.D.	N.D.	N.D.	Tuff from Mokulay stream outcrop.	N.D.		69.61982	88.33128
N12-8.2	C-580298	2.70	0.35	N.D.	N.D.	N.D.	Tuff from Mokulay stream outcrop.	N.D.		69.61982	88.33128
N12-8.3	C-580290	0.51	0.35	N.D.	N.D.	N.D.	Tuff from Mokulay stream outcrop.	N.D.		69.61982	88.33128
Angara River (earliest volcaniclastics, below lavas, southernmost region)											
A10-7.1	C-580297	0.71	0.30	1%	99%	0%	Tuff breccia with large stromatolitic blocks and small river pebbles.	N.D.	Fig. 3I; Figs. S2w, S2x	58.87805	102.37122
A10-8.2	C-580284	0.07	0.02	0%	60%	40%	Mafic clast in bedded lapilli tuff; sampled at waterline of 35-m-height outcrop.	N.D.		58.82252	102.53425
A10-9.1	C-580285	N.D.	0.57	70%	25%	5%	Volcaniclastic dike with abundant charcoal fragments.	Possibly high temperature		58.81039	102.56322
A10-11.1	C-580283	0.48	0.27	80%	20%	0%	Bedded accretionary lapilli–bearing lapilli tuff.	N.D.		58.79238	102.65560
A10-13.1	C-580282	0.21	0.01	0%	30%	70%	Cliff of bedded lapilli tuff on left bank of Kata River, 8–10 km from mouth on Angara River; organic and basaltic clasts; clasts both rounded and angular, lithic and juvenile. Accretionary lapilli 0.1–3 cm in diameter.	N.D.		58.73786	102.72170
A10-14.1	C-580289	N.D.	0.62	N.D.	N.D.	N.D.	1–1.5 km continuous river cliff of accretionary lapilli–bearing lapilli tuff and lapilli tuff with abundant small lithic clasts. Located on right side of Kata River, further west than site A10-13.	N.D.		58.76710	102.68647
A10-14.2	C-596833	0.75	0.36	80%	15%	5%	1–1.5 km continuous river cliff on right side of Kata River, further west than site A10-13. Faintly bedded lapilli tuff with sparse accretionary lapilli. Apparent charcoal pieces.	N.D.		58.76710	102.68647
Podkamennaya Tunguska River (pre-lava volcaniclastics, possibly reworked in explosion pipe, southernmost region)											
R06-12A	C-597436	1.08	0.21	0%	30%	70%	Lapilli tuff with predominantly juvenile clasts. Possibly reworked.	N.D.	Figs. 3G, 3H, 3 K; Fig. S2v	60.35750	99.9726
Kotuy River (volcaniclastics early in the lava sequence, northern region)											
K08-5.12	C-597437	0.37	0.02	N.D.	N.D.	N.D.	Lapilli tuff with juvenile clasts from the top of the first lava unit in the Arydzhangsky Formation.	N.D.		71.15095	102.673
K08-7.1	C-597438	N.D.	0.06	N.D.	N.D.	N.D.	Lapilli tuff with juvenile clasts from crack in top of flow ~35 m above Tunguska contact (cf. Fedorenko and Czamanske, 1997, their section 3).	N.D.		71.18120	102.58963
K08-7.4	C-597439	1.84	0.06	0%	100%	0%	Lapilli tuff with juvenile clasts in Fedorenko and Czamanske (1997, their section 3).	Sample K08-7.11, higher in the same sequence, is pyroclastic, 270 °C		71.18231	102.58999

Note: N.D.—no detection, or in the case of eruption temperature, not determined.
*Sample number in main collection, held by L.T. Elkins-Tanton at Arizona State University (Tempe, Arizona, USA).
†Analysis number in the lab of Stephen Grasby, Geological Survey of Canada (Calgary, Alberta, Canada).
§Bulk rock carbon content determined by ActLabs (Ancaster, Ontario, Canada) using IR.
#Total organic carbon determined by Rock-Eval6 (see the Supplemental Material [see text footnote 1]).
**Coal maceral type, as described in text, from lowest thermal alteration (T1) to highest (T3); expressed as a proportion of the total percentage of each maceral group to all macerals assemblage.
††Eruption temperature (*T*) estimated from paleomagnetism (Black et al., 2015).
§§See Figure 3 in text, and Figure S2 in the Supplemental Material (see text footnote 1).

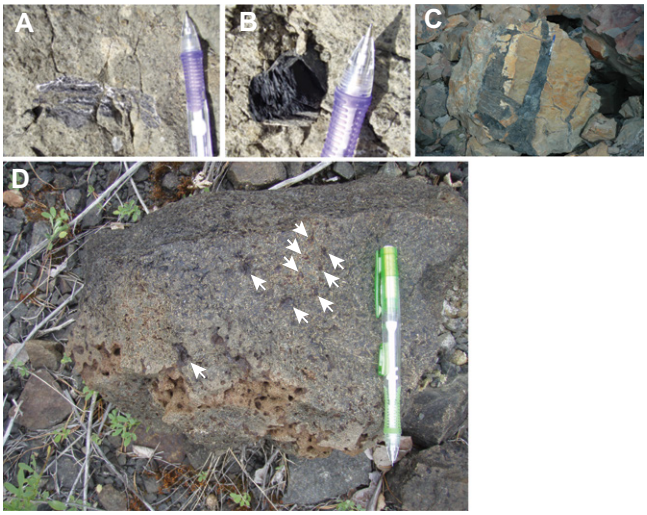

Figure 2. (A,B) Coaly and other organic pieces in volcaniclastics at sampling site NT12, Tura area (see Fig. 1 for location). (C) Liquefied coal injected into a displaced boulder from the Ivakinsky unit at the Kaerkan open-pit mine near the town of Talnakh, in the Norilsk region. (D) Small bituminous inclusions, soft to the fingernail, in coarse dolerite in the mine near Ust-Ilimsk (see Fig. 1 for location). Photos by L.T. Elkins-Tanton.

consist of vitrinite, with a mean R_{or} of 0.56% (Fig. S1A). These bituminous coal fragments likely reflect the level of thermal maturity prior to eruption and show devolatilization features such as small vacuoles and desiccation cracks (Figs. 3A–3D).

Type 2 macerals have bright high-temperature char rims surrounding a less-altered interior (Figs. 3G and 3H). These outer chars show R_{or} values as high as 4%, along with contraction cracks and combustion rims, and likely reflect combusted wood.

Type 3 macerals are cenospheres and char particles embedded in the volcaniclastic matrix (Figs. 3I–3N). Cenospheres are formed by explosive devolatilization of organic matter that was heated rapidly to high temperatures (~1300 °C; Goodarzi et al., 2008). We recognized two types: isotropic particles (Figs. 3I–3L) with plastic deformation and bright oxidation rims indicative of rapid heating in the presence of air (~30% of sampled cenospheres), and anisotropic particles (Figs. 3M and 3N) with a fine-grained optical texture typical of combustion byproducts of coal (Goodarzi and Hower, 2008) (Fig. S2).

DISCUSSION

Origins of Carbon-Rich Material within Siberian Volcanic Rocks

Of the eight volcaniclastic samples from the most southerly regions (the Podkamennaya Tunguska and Angara Rivers), seven contained coal and combusted organic-matter fragments. Abundant charcoal was also found in an end-Permian crater-lake deposit near Bratsk (Fristad et al., 2017). Only three of the eight samples from the Nizhnyaya Tunguska River, in central Siberia where the southernmost lavas appear, contain coal and organic matter. Farther north, only one of our six analyzed samples from the Norilsk and Kotuy regions contain coal and organic-matter fragments. However, previous work has identified graphite, bitumen, and carbonaceous material within Norilsk lavas and sills, which have been interpreted as evidence for incorporation of hydrocarbons in this area (e.g., Ryabov et al., 2012).

Near Norilsk, in the town of Kaerkan, a large open-pit coal mine contains outcrops where the Ivakinsky, the earliest lava flow, is in contact with coal. The coal appears to have been liquefied and injected into cracks in the cooling lava, leading to more-reducing conditions in the magma (e.g., Ryabov et al., 2014) (Fig. 2). Melenevsky et al. (2008) reported that coal in the broader aureole has been converted to anthracite, indicating heating to ~200 °C and release of ~260 kg HC/t organic matter (mass of hydrocarbon [HC] per unit mass of rock in metric tons). The southern volcaniclastics were also capable of burning or coking coal: paleomagnetic data demonstrating unidirectional remnant magnetization among some Angara rocks imply that temperatures exceeded 600 °C during magma emplacement (Black et al., 2015).

A major question is whether these samples record coal heated by magma, or incorporation of charcoal formed previously in wildfires (Grasby et al., 2015; Hudspith et al., 2014). Maceral texture distinguishes these options. We identify both isotropic high-reflectance organic matter (R_{or} >2% and as high as 11%), which may have resulted from forest fires, as well as high-reflectance chars with anisotropic cenospheres characteristic of coal combustion (Figs. 3M and 3N).

Cenospheres form in present-day coal-burning power plants (Hudspith et al., 2014). These particles are rarely reported in the pre-industrial sedimentary record, but have been observed in sedimentary rocks at the Permian-Triassic boundary in the Sverdrup Basin of Arctic Canada and are interpreted as a signature of magmatic coal combustion (Grasby et al., 2011), consistent with models of Ogden and Sleep (2012). In contrast, char and inertinite particles observed in our samples may be products of forest fires (e.g., Fristad et al., 2017) (Figs. 3I–3L).

Light-Carbon Release from Magma-Coal Interactions

The observations presented here are interpreted as evidence that coal and organic-matter combustion, along with forest fires, occurred in response to volcanism. Moreover, we infer that these interactions were widespread, based on the presence of thermally altered and/or burnt coal and organics in volcaniclastic rocks spanning the southern and central Siberian Traps province (Fig. 1).

The onset of the Permo-Triassic mass extinction is marked by a major carbon isotope excursion, which coincides within geochronological uncertainty with the oldest dated rocks from the Norilsk section (Burgess and Bowring, 2015). Emplacement of the organic matter–bearing southern volcaniclastic rocks preceded the main lava sequence (Levitan and Zastoina, 1985), permitting alignment with the carbon isotope excursion. Coincident with the isotope excursion, Siberian Traps magmatism was characterized by emplacement of laterally extensive sill complexes that could have facilitated significant interaction with coal and organic matter–bearing units (Burgess et al., 2017) and production of the volcaniclastic rocks.

Mantle carbon ($\delta^{13}C \approx -5‰$) (Javoy et al., 1986) and carbon in marine limestones ($\delta^{13}C \approx -2‰$ to $+2‰$) are too isotopically heavy to have caused the end-Permian carbon isotope excursion (e.g., Cui and Kump, 2015; Gales et al., 2020; Payne and Kump, 2007). Consequently, coal or organic matter ($\delta^{13}C \approx -25‰$) (Cui et al., 2013), methane clathrates ($\delta^{13}C \approx -56‰$) (Krull and Retallack, 2000), or petroleum ($\delta^{13}C \approx -30‰$ to $-25‰$) (Svensen et al., 2009) represent the most plausible sources of light-carbon injection. Assuming equilibrium with an end-Permian dissolved inorganic carbon (DIC) reservoir of 38,000 Gt C with an initial DIC $\delta^{13}C = 0$, and a C isotope mass balance in which $\Delta^{13}C = \Delta M * \delta^{13}C_{coal} / (\Delta M + DIC)$, where $\Delta^{13}C$ denotes the magnitude of the isotope excursion and ΔM denotes C release from coal, we infer that each 1000 Mt C released from coal or organic matter with $\delta^{13}C_{coal} \approx -25‰$ would translate to an ~–0.64‰ shift in ocean-atmosphere $\delta^{13}C$ (Cui and Kump, 2015). Mass-balance calculations indicate that 6000–10,000 Gt C with $\delta^{13}C \approx -25‰$ could yield a global carbon isotope perturbation with the observed magnitude of −3‰ to −6‰ (Cui and Kump, 2015).

The primary uncertainties for estimating the magnitude of light-carbon release are (1) the total mass of coal and organic matter that interacted with Siberian Traps magmas and (2) the efficiency of carbon release to the atmosphere during these interactions. The cumulative thickness of Carboniferous to Permian coal layers in the Tunguska Basin has been estimated as ~100 m (Retallack and Jahren, 2008),

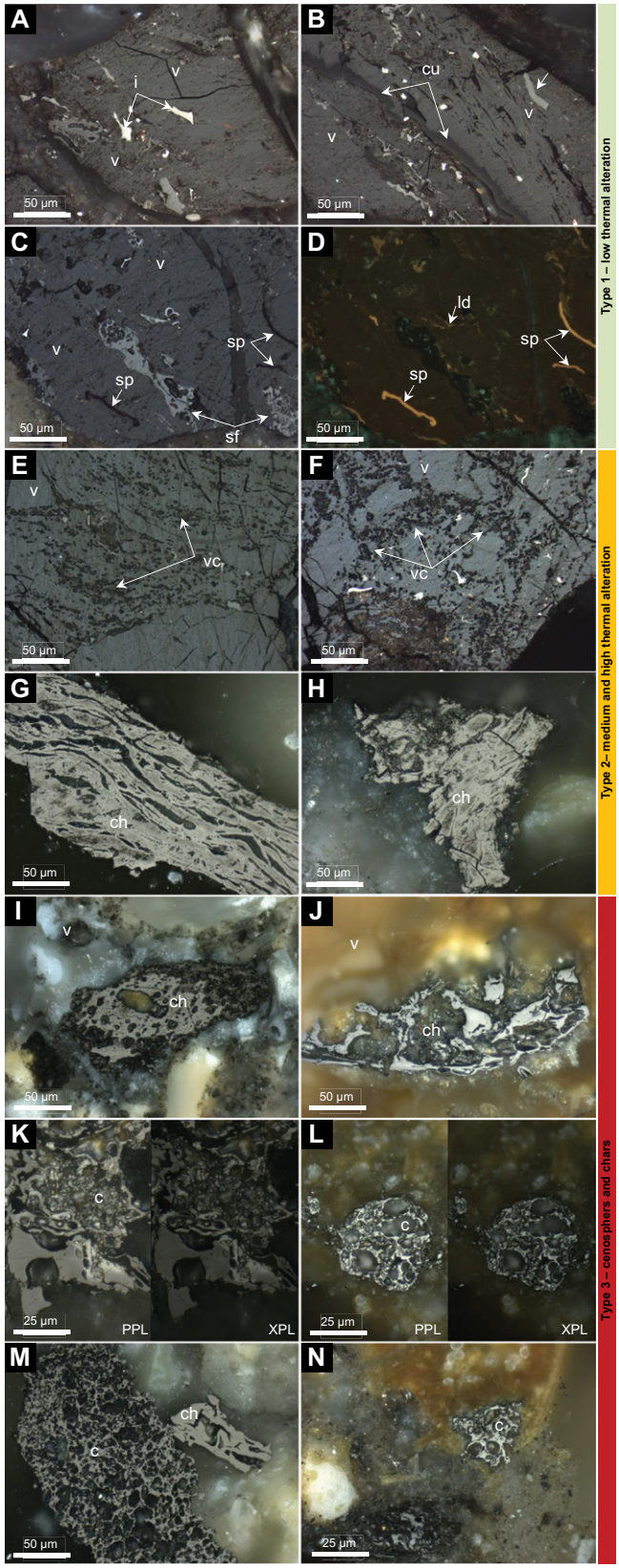

Figure 3. Photomicrographs of macerals taken under reflected white light and oil immersion; 50× objective unless specified. (A–C) Low thermal alteration (random vitrinite reflectance R_{or} = 0.56%) of coal fragments of vitrinite (v), semi fusinite (sf), inertinite (i), cutinite (cu), sporinite (sp), and liptodetrinite (ld). All vitrinite particles show features of low thermal alteration such as minor dehydration fracturing. (D) Sample from C under ultraviolet light. Orange-fluorescing macerals (e.g., sp and ld) indicate low thermal maturity coal fragments. (E–F) Vitrinite particles (R_{or} = 0.83%) with desiccation cracks and vacuoles suggesting higher temperatures and devolatilization. (G–H) Highly thermally altered particles from plants (ch—char). Bright rim and internal structures are evidence of high-temperature combustion. (I–J) High-temperature char (ch) particles with fine devolatilization vacuoles and granular texture. Mean R_{or} = ~4%. (K–L) Isotropic cenospheric (c) and char (ch) particles with devolatilization vacuoles and fine granular texture and high reflectance (6%–10%). (M–N) Cenospheres with anisotropy due to elevated temperatures. Right images in M and N were taken with cross polarized light (XPL); all others were taken in plane polarized light (PPL). Images A–D, M, and N are from sample NT12-6.2; E and F are from sample NT12-4.3; G and H are from sample R06-12A; I is from sample A10-7.1; J is from sample A10-14.2; K is from sample R06-12A; L is from sample NT12-6.2.

comprising ~10^4–10^5 Gt C. Thermodynamic and experimental data (Iacono-Marziano et al., 2012) suggest that coal combustion and/or coking takes place only at pressures of several hundred bars or less, and at the onset of Siberian magmatism, Permian coal measures were indeed located near the surface (Retallack and Jahren, 2008). We interpret some of the combusted particles as originating from organic matter rather than mature coal, and the mass of organic matter hosted in organic-rich shales and peats in the Tunguska Basin is much larger than that of coal proper (Svensen et al., 2009), suggesting that ~10^4–10^5 Gt C represents a lower estimate of carbon available, sufficient to drive the observed carbon isotope excursion based on the mass-balance calculations discussed above.

CONCLUSIONS

Our findings provide direct field evidence that Siberian Traps magmas incorporated and combusted coal and organic-rich material. This combustion may have been linked to the formation of breccia pipes in the region (Jerram et al., 2016; Ogden and Sleep, 2012; Svensen et al., 2009). The presence of cenospheres and char also provides evidence for ejection of combusted coal ash into the atmosphere, supporting previous suggestions of significant coal fly ash formation at this time in Siberia, carried on global air currents and deposited in the Arctic Canada Sverdrup Basin (Grasby et al., 2011). In addition to carbon released from the mantle (Sobolev et al., 2011) and thermally metamorphosed country rocks, our results show that coal combustion also liberated light carbon, contributing to the global warming and carbon-cycle disruption that characterized the Permo-Triassic mass extinction (e.g., Cui and Kump, 2015).

ACKNOWLEDGMENTS

We thank reviewers Paul Wignall, Henrik Svensen, and Ying Cui, and our team members. Funding was provided by U.S. National Science Foundation (NSF) Continental Dynamics grant EAR-0807585 to Elkins-Tanton, a grant of the Russian Foundation for Basic Research (18-35-20058) to Veselovskiy, and NSF Integrated Earth Systems grant EAR-1615147 to Black.

REFERENCES CITED

Black, B.A., Weiss, B.P., Elkins-Tanton, L.T., Veselovskiy, R.V., and Latyshev, A.V., 2015, Siberian Traps volcaniclastic rocks and the role of magma-water interactions: Geological Society of America Bulletin, v. 127, p. 1437–1452, https://doi.org/10.1130/B31108.1.

Black, B.A., Neely, R.R., Lamarque, J.-F., Elkins Tanton, L.T., Kiehl, J.T., Shields, C.A., Mills, M.J., and Bardeen, C., 2018, Systemic swings in end-Permian climate from Siberian Traps carbon and sulfur degassing: Nature Geoscience, v. 11, p. 949–954, https://doi.org/10.1038/s41561-018-0261-y.

Burgess, S.D., and Bowring, S.A., 2015, High-precision geochronology confirms voluminous magmatism before, during, and after Earth's most severe extinction: Science Advances, v. 1, e1500470, https://doi.org/10.1126/sciadv.1500470.

Burgess, S.D., Muirhead, J.D., and Bowring, S.A., 2017, Initial pulse of Siberian Traps sills as the trigger of the end-Permian mass extinction: Nature Communications, v. 8, 164, https://doi.org/10.1038/s41467-017-00083-9.

Cui, Y., and Kump, L.R., 2015, Global warming and the end-Permian extinction event: Proxy and modeling perspectives: Earth-Science Reviews, v. 149, p. 5–22, https://doi.org/10.1016/j.earscirev.2014.04.007.

Cui, Y., Kump, L.R., and Ridgwell, A., 2013, Initial assessment of the carbon emission rate and

climatic consequences during the end-Permian mass extinction: Palaeogeography, Palaeoclimatology, Palaeoecology, v. 389, p. 128–136, https://doi.org/10.1016/j.palaeo.2013.09.001.
Erwin, D.H., 2006, Extinction: How Life Nearly Died 250 Million Years Ago: Princeton, New Jersey, Princeton University Press, 296 p.
Fedorenko, V.A., and Czamanske, G.K., 1997, Results of new field and geochemical studies of the volcanic and intrusive rocks of the Maymecha-Kotuy area, Siberian flood-basalt province, Russia: International Geology Review, v. 39, p. 479–531, https://doi.org/10.1080/00206819709465286.
Fristad, K.E., Svensen, H.H., Polozov, A.G., and Planke, S., 2017, Formation and evolution of the end-Permian Oktyabrsk volcanic crater in the Tunguska Basin, Eastern Siberia: Palaeogeography, Palaeoclimatology, Palaeoecology, v. 468, p. 76–87, https://doi.org/10.1016/j.palaeo.2016.11.025.
Gales, E., Black, B., and Elkins-Tanton, L.T., 2020, Carbonatites as a record of the carbon isotope composition of large igneous province outgassing: Earth and Planetary Science Letters, v. 535, 116076, https://doi.org/10.1016/j.epsl.2020.116076.
Goodarzi, F., and Hower, J.C., 2008, Classification of carbon in Canadian fly ashes and their implications in the capture of mercury: Fuel, v. 87, p. 1949–1957, https://doi.org/10.1016/j.fuel.2007.11.018.
Goodarzi, F., Huggins, F.E., and Sanei, H., 2008, Assessment of elements, speciation of As, Cr, Ni and emitted Hg for a Canadian power plant burning bituminous coal: International Journal of Coal Geology, v. 74, p. 1–12, https://doi.org/10.1016/j.coal.2007.09.002.
Grasby, S.E., Sanei, H., and Beauchamp, B., 2011, Catastrophic dispersion of coal fly ash into oceans during the latest Permian extinction: Nature Geoscience, v. 4, p. 104–107, https://doi.org/10.1038/ngeo1069.
Grasby, S.E., Sanei, H., and Beauchamp, B., 2015, Latest Permian chars may derive from wildfires, not coal combustion: Comment: Geology, v. 43, p. e358, https://doi.org/10.1130/G36539C.1.
Hudspith, V.A., Rimmer, S.M., and Belcher, C.M., 2014, Latest Permian chars may derive from wildfires, not coal combustion: Geology, v. 42, p. 879–882, https://doi.org/10.1130/G35920.1.
Iacono-Marziano, G., Marecal, V., Pirre, M., Gaillard, F., Arteta, J., Scaillet, B., and Arndt, N.T., 2012, Gas emissions due to magma-sediment interactions during flood magmatism at the Siberian Traps: Gas dispersion and environmental consequences: Earth and Planetary Science Letters, v. 357, p. 308–318, https://doi.org/10.1016/j.epsl.2012.09.051.
Il'yukhina, N.P., and Verbitskaya, N.G., 1976, Formation conditions and stratigraphy of Carboniferous coal deposits of the Siberian platform: International Geology Review, v. 19, p. 429–440, https://doi.org/10.1080/00206817709471037.
Javoy, M., Pineau, F., and Delorme, H., 1986, Carbon and nitrogen isotopes in the mantle: Chemical Geology, v. 57, p. 41–62, https://doi.org/10.1016/0009-2541(86)90093-8.
Jerram, D.A., Svensen, H.H., Planke, S., Polozov, A.G., and Torsvik, T.H., 2016, The onset of flood volcanism in the north-western part of the Siberian Traps: Explosive volcanism versus effusive lava flows: Palaeogeography, Palaeoclimatology, Palaeoecology, v. 441, p. 38–50, https://doi.org/10.1016/j.palaeo.2015.04.022.
Krull, E.S., and Retallack, G.J., 2000, $\delta^{13}C$ depth profiles from paleosols across the Permian-Triassic boundary: Evidence for methane release: Geological Society of America Bulletin, v. 112, p. 1459–1472, https://doi.org/10.1130/0016-7606(2000)112<1459:CDPFPA>2.0.CO;2.
Levitan, M.M., and Zastoina, A.N., 1985, Federal Geological Map of USSR: Leningrad, VSEGEI, scale 1:100,000.
Malich, N.S., et al., 1974, Map of geological formations of the Siberian platform cover: Leningrad, VSEGEI, scale 1:1,500,000.
Melenevsky, V.N., Fomin, A.N., Konyshev, A.S., and Talibova, O.G., 2008, Contact coal transformation under the influence of dolerite dike (Kaierkan deposit, Noril'sk district): Russian Geology and Geophysics, v. 49, p. 667–672, https://doi.org/10.1016/j.rgg.2008.01.007.
Naumov, V.A., and Ankudimova, L.A., 1995, Palynocomplexes and age of volcanogenic deposits of the Angara-Katanga area (Middle Angara Region): Geologiya Geofizica, v. 36, p. 39–45.
Ogden, D.E., and Sleep, N.H., 2012, Explosive eruption of coal and basalt and the end-Permian mass extinction: Proceedings of the National Academy of Sciences of the United States of America, v. 109, p. 59–62, https://doi.org/10.1073/pnas.1118675109.
Payne, J.L., and Clapham, M.E., 2012, End-Permian mass extinction in the oceans: An ancient analog for the twenty-first century?: Annual Review of Earth and Planetary Sciences, v. 40, p. 89–111, https://doi.org/10.1146/annurev-earth-042711-105329.
Payne, J.L., and Kump, L.R., 2007, Evidence for recurrent Early Triassic massive volcanism from quantitative interpretation of carbon isotope fluctuations: Earth and Planetary Science Letters, v. 256, p. 264–277, https://doi.org/10.1016/j.epsl.2007.01.034.
Permyakov, S.A., et al., 2012, State Geological Map of the Russian Federation, Scale 1:1000000, (third generation): Angaro-Yeniseyskaya Series (O-48 - Ust'-Ilimsk), Explanatory Notes: Saint Petersburg, VSEGEI, 433 p.
Peters, K.E., and Cassa, M.R., 1994, Applied source rock geochemistry, *in* Magoon, L.B., and Dow, W.G., eds., The Petroleum System—From Source to Trap: American Association of Petroleum Geologists Memoir 60, p. 93–120, https://doi.org/10.1306/M60585C5.
Retallack, G.J., and Jahren, A.H., 2008, Methane release from igneous intrusion of coal during Late Permian extinction events: The Journal of Geology, v. 116, p. 1–20, https://doi.org/10.1086/524120.
Ryabov, V.V., Ponomarchuk, V.A., Titov, A.T., and Semenova, D.V., 2012, Micro- and nanostructures of carbon in Pt-low-sulfide ores of the Talnakh deposit (Siberian platform): Doklady Earth Sciences, v. 446, p. 1193–1196, https://doi.org/10.1134/S1028334X12100121.
Ryabov, V.V., Shevko, A.Y., and Gora, M.P., 2014, Trap Magmatism and Ore Formations in the Siberian Noril'sk Region, Volume 1: Trap Petrology: Dordrecht, Springer, Modern Approaches in Solid Earth Sciences, v. 3, 390 p.
Sobolev, S.V., Sobolev, A.V., Kuzmin, D.V., Krivolutskaya, N.A., Petrunin, A.G., Arndt, N.T., Radko, V.A., and Vasiliev, Y.R., 2011, Linking mantle plumes, large igneous provinces and environmental catastrophes: Nature, v. 477, p. 312–316, https://doi.org/10.1038/nature10385.
Svensen, H., Planke, S., Polozov, A.G., Schmidbauer, N., Corfu, F., Podladchikov, Y.Y., and Jamtveit, B., 2009, Siberian gas venting and the end-Permian environmental crisis: Earth and Planetary Science Letters, v. 277, p. 490–500, https://doi.org/10.1016/j.epsl.2008.11.015.
Svensen, H.H., Frolov, S., Akhmanov, G.G., Polozov, A.G., Jerram, D.A., Shiganova, O.V., Melnikov, N.V., Iyer, K., and Planke, S., 2018, Sills and gas generation in the Siberian Traps: Philosophical Transactions of the Royal Society A: Mathematical, Physical, and Engineering Sciences, v. 376, 20170080, https://doi.org/10.1098/rsta.2017.0080.
Wignall, P.B., 2001, Large igneous provinces and mass extinctions: Earth-Science Reviews, v. 53, p. 1–33, https://doi.org/10.1016/S0012-8252(00)00037-4.

Printed in USA